

# Constitution and corrosion resistance of phosphate protective coatings

GIUSEPPINA ACQUARONE, EMMA ANGELINI, PAOLO BIANCO, GIANFRANCA GRASSI  
Dipartimento di Scienza dei Materiali e Ingegneria Chimica, Politecnico di Torino

## Abstract

*Various protective coatings obtained by phosphating were examined in order to establish the interdependence between the constitution of the coating and such electrochemical properties as can be related to corrosion resistance, in particular free corrosion potential and polarization resistance.*

## Riassunto

### Costituzione e resistenza alla corrosione di strati protettivi fosfatati

Sono stati esaminati diversi tipi di rivestimento protettivo ottenuto per fosfatazione con riferimento alle correlazioni esistenti tra costituzione dello strato e caratteristiche elettrochimiche di resistenza alla corrosione, quali in particolare i potenziali di libera corrosione e la resistenza di polarizzazione.

## Introduction

The surface conversion of steel by means of a phosphate coating promotes better adhesion of the subsequent coatings and inhibits detachment in a corrosive environment, which is usually caused by cuts and other defects (1, 2).

Phosphatizing processes based on zinc phosphate, applied by spray or immersion, have been developed in order to produce coatings in relatively short times.

The ever growing need for reliable and long-lasting industrial products, and harder service conditions, especially in the motor-car industry, due to both the atmospheric pollution and the use of de-icing salts on the road, has prompted research into new surface protection technologies with an aim at improving the corrosion resistance of products.

The newly developed immersion phosphating processes produce precipitates which are rich in phosphophyllite crystals as a result of the reduced diffusion rate of the ferrous ions within the boundary layer  $[\text{Zn}_2(\text{Fe}^{2+}, \text{Mn})(\text{PO}_4)_2 \cdot 4\text{H}_2\text{O}]$ . On the other hand, in the case of spray coating, the boundary layer is much reduced because of the high turbulence level and the ferrous ions pass into solution, where are oxidized and precipitated into slurry in the form of hureaulite  $[\text{Fe}_5\text{H}_2(\text{PO}_4)_4 \cdot 4\text{H}_2\text{O}]$  or strengite  $[\text{FePO}_4 \cdot 2\text{H}_2\text{O}]$  the phosphate coating consisting mainly of hopeite  $[\text{Zn}_3\text{PO}_4 \cdot 4\text{H}_2\text{O}]$  (1, 3, 4).

This paper aims at assessing the influence of crystalline phases on the characteristics of phosphate coatings obtained by immersion and spray processes.

The corrosion resistance of specimens phosphated and subsequently coated with a cathaphoretic primer has also been assessed, the anti-corrosive protection being provided by the combination of the two treatments.

## Materials and methodologies

A UNI C 7 deep-drawing plate was used having the following characteristic: C 0.065; Mn 0.24; Cu 0.025; Al 0.05; P 0.014; S 0.015. The surface C content was  $1.8 \text{ mg/m}^2$  which was determined according to Ford's method (5); roughness was  $R_a = 1.7$ .

The  $70 \times 150 \text{ mm}$  specimens were degreased in an alkaline bath at  $75^\circ\text{C}$  for 15 minutes. (NaOH 6%,  $\text{Na}_2\text{CO}_3$  2%,  $\text{Na}_2\text{SiO}_3$  2%, Sodium gluconate 5%, surfactant (Ambrim) 0.2%) and then phosphated using various baths and application techniques, as shown in Table 1.

Some of the phosphated specimens were given a  $25 \mu\text{m}$  thick coating with a cathaphoretic primer, before undergoing corrosion tests.

After the phosphating treatment, the specimens were examined by means of x-Ray diffractometry ( $\text{FeK } \alpha$ ,  $\lambda_{\alpha} = 0.19374 \text{ nm}$ ).

The existing phases could not be evaluated quantitatively because of the thin phosphate coating and the preferential orientation of the phosphate crystals on the metallic surfaces with consequent predominance of reflections from the lattice planes (100) and (020), (6).

The X-ray examination confirmed that hopeite and phosphophyllite are the main mineralogical components of the film adhering to the steel. Their relative quantity was measured on the basis of the integrated intensities of the peaks of the abovementioned phases and in accordance with data in the literature (7).

Due to the reduced thickness of the phosphate coating, only the reflections from low angles incident radiation could be measured in a meaningful way; therefore a quantitative X-ray examination based on peak area



**TABLE 1**

Product	Application	Length of time	After treatment
1. Zn/Mn (a) cold, self-accelerated phosphating agent	spray	180"	drying T = 110°C, 10 min
2. Zn/Mn (b) cold, self-accelerated phosphating agent	spray	180"	drying T = 110°C, 10 min
3. Zn/Ni hot phosphating agent, 50-55°C temperature, nitrites/nitrates accelerated	immersion	180"	drying T = 110°C, 10 min.
4. Zn/Ni hot phosphating agent, 50-55°C temperature, nitrites/nitrates accelerated	immersion	180"	drying T = 110°C, 10 min and chromic passivation
5. Zn/Ni hot phosphating agent, 50-55°C temperature, nitrites/nitrates accelerated	spray/ immersion	180"	drying T = 110°C, 10 min.

measurement could not be carried out.

The "coating weight" (that is the weight increase per surface unit which follows from the phosphate coating treatment) is often the only parameter used for assessing coatings. It was determined, after removal of the phosphated layer, by immersion in a chromic acid solution (100 g/l) at 75°C (8) for 15 minutes. Then, the  $Zn^{2+}$  and  $Fe^{2+}$  concentrations of the etching solution were determined by atomic absorption spectrophotometry in order to correlate the Fe/Zn and phosphophyllite/hopeite ratios, the other phases being, by comparison, negligible.

Electron microscopy techniques (SEM) were used for evaluating both the crystals morphology and the substrate coating.

A potentiostat equipped with a function generator and linked to an X-Y recorder was used for determining the electrochemical characteristics of the phosphate coatings.

The polarization resistance,  $R_p$ , which is inversely proportional to the corrosion rate, was measured in a phosphate-aggressive medium ( $NH_4NO_3$  0.6 M). After superposing a 20 mV, 5mHz triangular wave potential to the free corrosion potential, the consequent current variations were measured in order to evaluate the corrosion resistance from the tendency to the stability of the free corrosion potential when polarization occurs at the specimen surface.

As the correlation between resistance to corrosion in the salt spray test after the application of the primer and the porosity of the phosphate coating had been pointed out by several authors (8,9) particular attention was given to the problem. In this connection three methods taken from the literature were found to be useful.

The first method (9) is based on the reduction reaction of the oxygen dissolved in the test solution, NaOH, pH

= 12. As this reaction takes place on active cathodic areas only, it would appear that the reduction current is related to porosity. Reduction was obtained by cathodic polarization of the phosphated specimens from the equilibrium potential up to -1.1 V (SCE), the scanning rate being 2mV/s. The reduction current density was measured at -0.55 V (SCE) and the maximum differentiation between the various coatings should be found at this potential. One of the drawbacks of this method is that the extremely alkaline electrolyte etches and dissolves the zinc phosphates, thus causing continuous surface modification. For this reason the current density was also measured in an NaCl 3% solution at -1 V (SCE), where the rate of dissolution of iron is minimal (8).

Finally, the porosity of the layers can be assessed optically by electrophoresis of a dye, that is by anodic treatment of the specimens in a solution consisting of 2.5 g/l alizarin-sulphonic acid sodium salt and 80 g/l hexamethylene tetramine, with cell potential of 3 V. The dye precipitates onto the uncoated metallic areas so that the number and areas of the pores can be measured by microscope examination (10).

The corrosion resistance of specimens phosphated and coated with cathaphoretic primer was evaluated by means of salt spray (11) and filiform corrosion tests. As for the latter, the initiation of corrosion was obtained by scratching, then coating with Corrodokote paste (12) and keeping them for 24 hours at 100% relative humidity at 30°C. After removal of the paste the specimens were introduced into a chamber with a constant humidity level, 87% relative humidity and a temperature of 30°C and the corrosion was measured at 250 hours intervals. After the salt spray test the primer film was removed and the spread of corrosion measured.



**TABLE 2**

Tests	Specimens				
	1	2	3	4	5
Coating weight (g/m <sup>2</sup> )	0.98	3.80	1.98	2.36	2.33
Phosphophyllite proportion	0.219	0.154	1.00	0.542	0.372
Porosity (alizarin S) (pores/cm <sup>-2</sup> 10 <sup>3</sup> )	2.11	2.83	11.0	2.30	3.56
Free corrosion potential, NaOH, pH = 12 [V(SCE)]	- 0.223	- 0.265	- 0.156	- 0.145	- 0.180
Free corrosion potential, NaCl 3% [V(SCE)]	- 0.479	- 0.504	- 0.443	- 0.407	- 0.397
Free corrosion potential, NH <sub>4</sub> NO <sub>3</sub> 0.6M, 3' [V(SCE)]	- 0.625	- 0.601	0.020	0.014	- 0.614
Free corrosion potential, NH <sub>4</sub> NO <sub>3</sub> 0.6M, 30' [V(SCE)]	- 0.616	- 0.609	- 0.232	- 0.628	- 0.641
Reduction O <sub>2</sub> in NaOH at V = - 0.55 V (SCE) [i(μA/cm <sup>-2</sup> )]	11.3	1.45	7.50	7.30	5.85
Reduction O <sub>2</sub> in NaCl 3%, at V = - 1 V (SCE) [i(μA/cm <sup>-2</sup> )]	25.3	16.0	17.6	19.6	26.0
Polarization resistance in NH <sub>4</sub> NO <sub>3</sub> 0.6M, 3' (k Ω cm <sup>2</sup> )	0.259	2.79	14.06	12.50	0.357
Polarization resistance in NH <sub>4</sub> NO <sub>3</sub> 0.6M, 30' (k Ω cm <sup>2</sup> )	1.043	3.82	0.294	0.561	0.810
Filiform corrosion, 750 hrs (mm from etch)	2.3	6.8	2.0	2.0	5.0
Salt spray corrosion, 700 hrs (mm from etch)	3.0	3.0	1.0	1.5	1.5

## Results and discussion

Table 2 shows the result of the various tests. The morphological examination of the phosphated surfaces agreed with the data from the X-ray examination but the existing phases could not be determined unequivocally. Specimens 1 and 2 (Fig. 1) present the oriented lamella structure of hopeite which is their main component. Specimens 3 and 4 (Fig. 2) were obtained by the immersion process, and show a uniform coating of "non-oriented" phosphophyllite coarse crystals. Specimen 5 (Fig. 3) was obtained by spray-immersion treatment: it combines crystals of uncertain origin with un-oriented phosphophyllite crystals (4).

It is worth mentioning that Specimen 4 appears coated with phosphophyllite but the X-ray diffraction results show it to have a high hopeite percentage with a low intensity peak. This is due to the dissolution and precipitation of products during passivation.

The results of the tests were correlated in order to evaluate the influence of the characteristics of the phosphated coatings (phosphophyllite/hopeite ratio, coating weight, etc.) on the coatings' corrosion resistance.

The coating weight, which is expressed in terms of the oxygen reduction current density in NaOH, pH = 12, gives an average line from the experimental results with high correlation coefficient ( $r = -0.987$ ) (Fig. 4). Similar correlations cannot be found when taking into consideration the data offered by the two other methods used for determining the porosity level. We can understand this result better if we suppose that the electrolyte attacks the phosphate coating so that the oxygen reduction takes place not only in the pores but also on the metallic surface which becomes exposed by the dissolution of the phosphates. As a consequence, the reduction current will be greater on thinner coatings, the initial porosity being equal. Interesting correlations can be found, on the other

Fig. 1 - SEM micrographies of specimens 1 and 2; phosphate coatings with hopeite structure) 1, 2 (500 ×); 1', 2' (2500 ×).





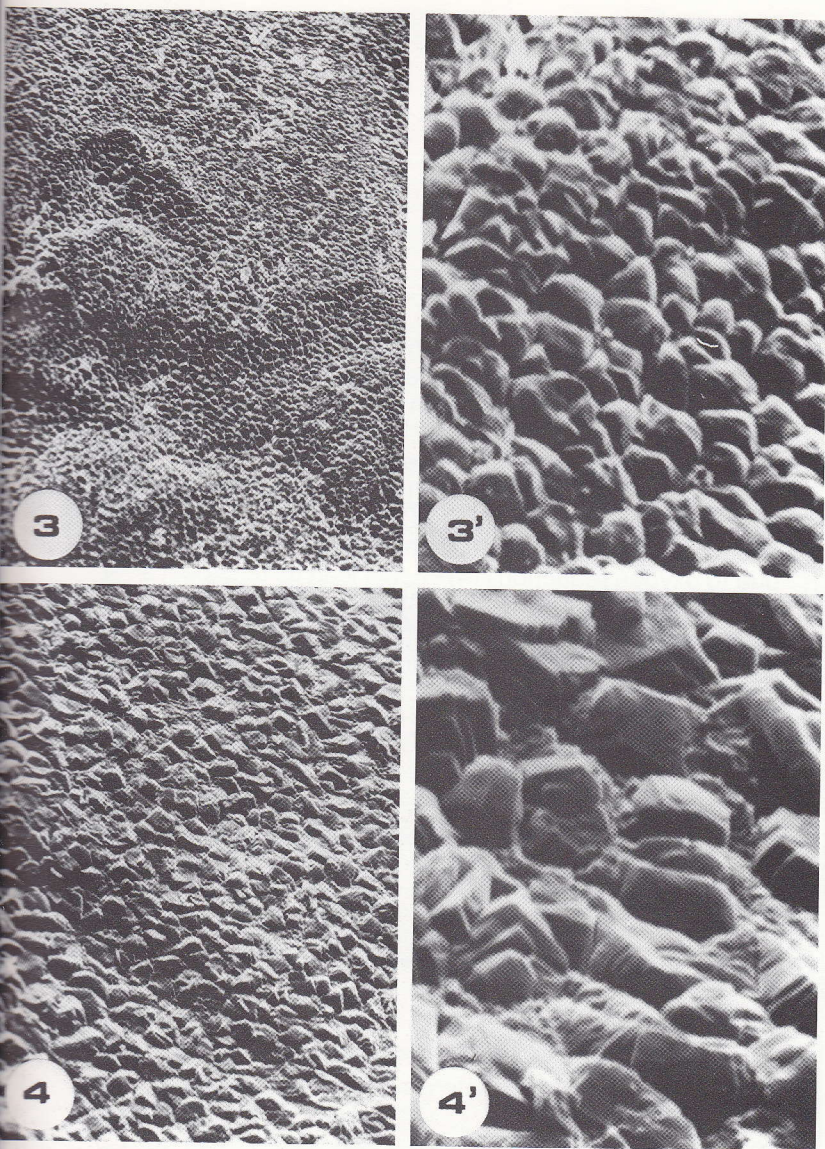


Fig. 2 - SEM micrographs of specimens 3 and 4; phosphate coatings with unoriented phosphophyllite structure; 3, 4 (500  $\times$ ); 3', 4' (2500  $\times$ ).

Fig. 3 - SEM micrographs of specimen 5; phosphate coating made of unoriented phosphophyllite crystals and crystals of uncertain origin; 5 (500  $\times$ ); 5' (2500  $\times$ ).

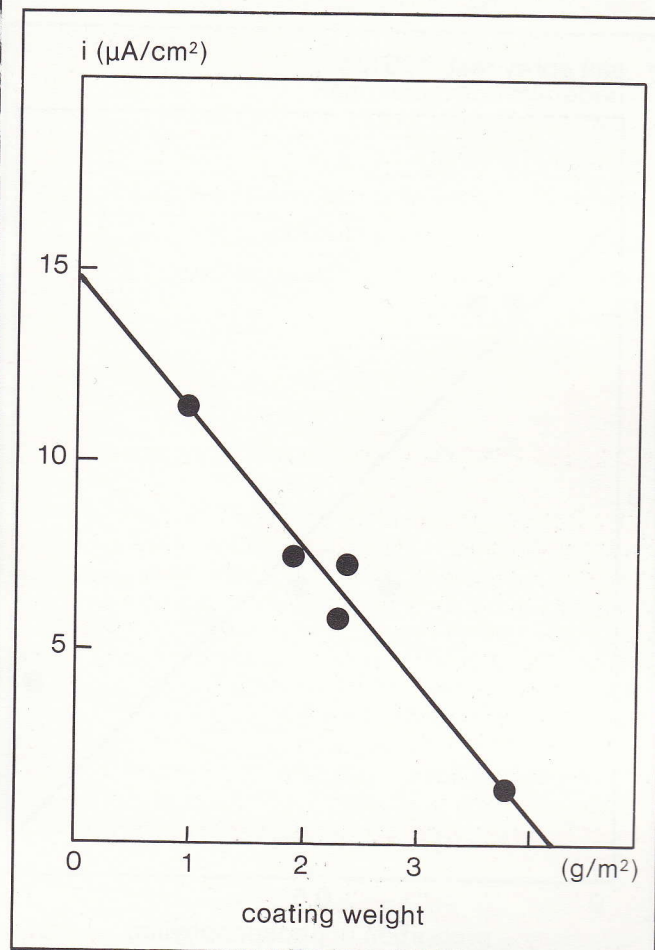
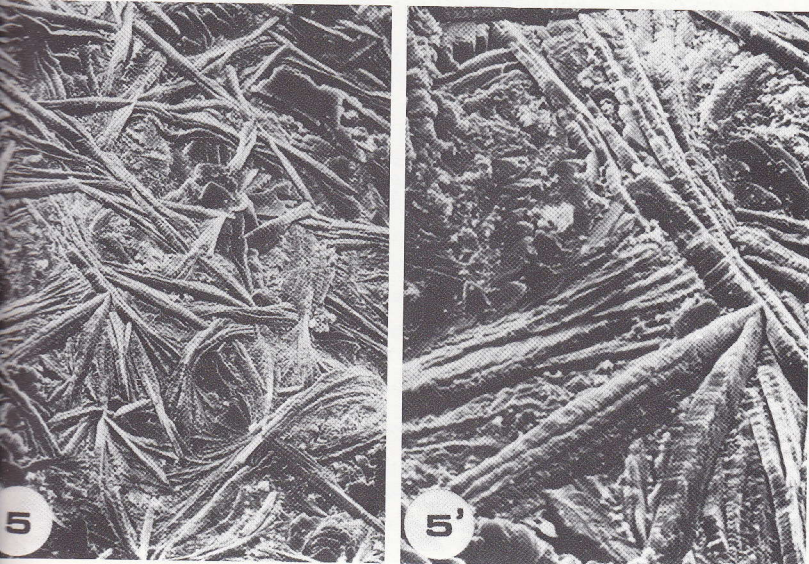


Fig. 4 - Correlation between coating weight and oxygen reduction current density in NaOH solution, pH = 12.

hand, between the proportion of phosphophyllite and the free corrosion potentials of the specimens in the various test solutions. The higher the phosphophyllite content of the phosphate coating the nobler the potentials (Table 2).

The fact that coatings with high phosphophyllite content tend to assume a more positive free corrosion potential is also shown by tests carried out in  $\text{NH}_4\text{NO}_3$  for determining the polarization resistance,  $R_p$ . Phosphophyllite-rich specimens assumed potentials which are very close to zero ( $\sim 20\text{mV}$ ) reaching  $-0.6\text{V}$  (SCE) in 30 minutes' time; hopeite-rich coatings reached  $-0.6\text{V}$  (SCE) values in the first 3 minutes' immersion.

These measurements take place in a phosphate-aggressive environment, the phosphates being, at least partially, soluble in ammonium salt solutions (13). Therefore it can be presumed that phosphophyllite layer has better corrosion resistance and gives longer protection to the substrate. Hopeite, on the other hand,



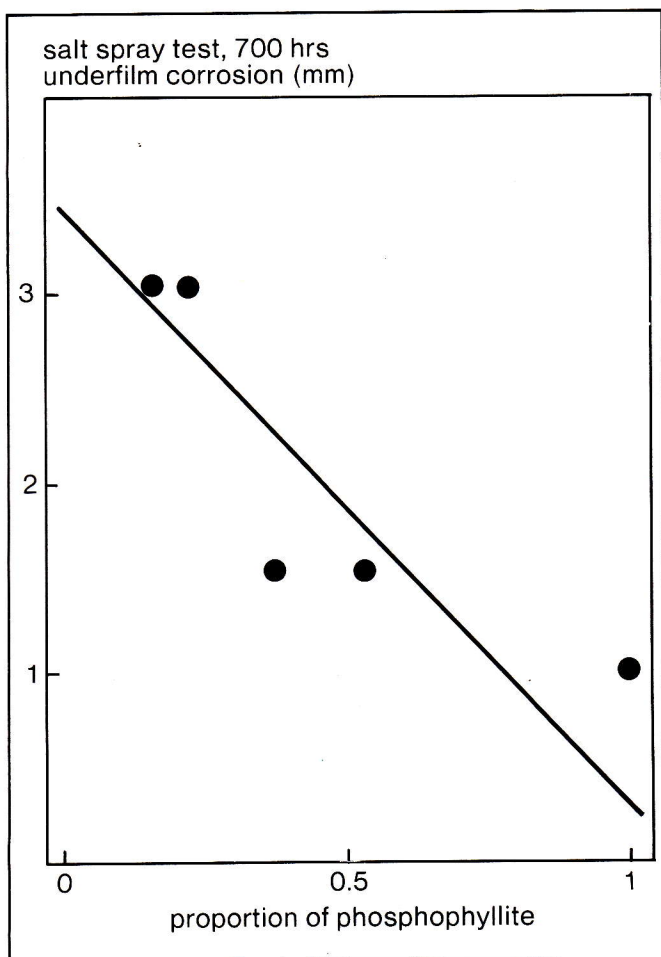


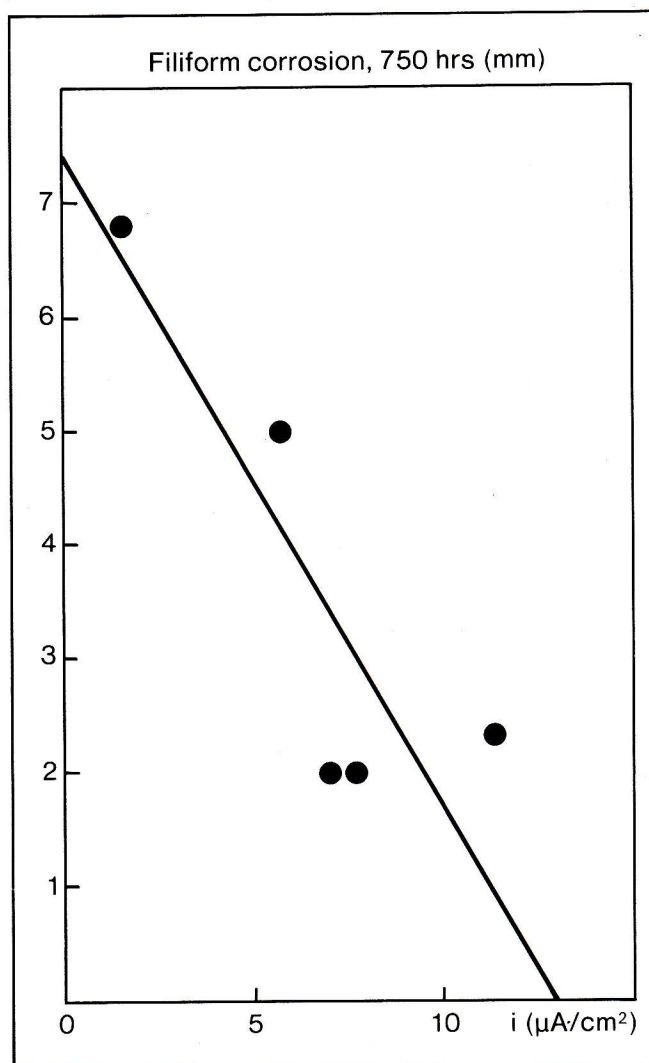
Fig. 5 - Correlation between phosphophyllite proportion in the phosphate coating and underfilm corrosion after salt spray test, 700 hrs.

is immediately attacked and the specimen takes the typical free corrosion potential of the uncovered metallic surface. This hypothesis is confirmed by the polarization resistance values which were measured after 3 minutes' immersion. Very high values and, consequently, low corrosion rate, were registered for specimens 3 and 4, whereas after stabilisation of the potentials (30 minutes' immersion) the polarization resistance had the same value for all specimens. In this assessment specimen 2 was an exception, probably because of the very thick conversion layer.

Fig. 5 presents the correlation between the phosphophyllite proportion and the underfilm corrosion of cathodically coated specimens after 700 hours salt-spray test ( $r = -0.856$ ). It can be seen that phosphophyllite greatly improves the corrosion resistance characteristics after painting.

The three methods employed for evaluating the phosphate coating porosity gave discordant results which cannot be correlated with either the existing crystalline phases or other data. A high correlation coefficient ( $r = -0.845$ ) can be detected only between the current density of the oxygen reduction in NaOH and the filiform corrosion after 750 hours testing. The fact that the cathodic current in filiform corrosion is due to oxygen reduction (14) should lead us to expect a smaller amount of corrosion in specimens with smaller oxygen reduction current. Results, however, prove that this test is not significant (Fig. 6).

Fig. 6 - Correlation between oxygen reduction current density in NaOH solution, pH = 12, and filiform corrosion spread, 750 hrs.



## Conclusion

The following conclusions can be drawn from the tests performed:

- 1 - The nobler values of the free corrosion potentials and the higher polarization resistance show that phosphophyllite coatings offer improved corrosion resistance.
- 2 - These characteristics lead not only to increased primer adhesion but also to higher corrosion resistance after primer painting, as salt spray and filiform corrosion tests have shown.

## REFERENCES

- (1) Machu W., *La fosfatazione dei metalli* Hoepli, Milano, 1955.
- (2) Cheever G.D. The chemistry of zinc phosphate coatings. *SAE Paper*, 700460 (1970).
- (3) Falcone P. Stato della ricerca e della affidabilità dei prodotti e dei cicli di pretrattamento alla luce delle nuove esigenze qualitative di anticorrosione. *Verniciatura Industriale*, 15 (1982), 114.
- (4) Fosfacol S.p.A., *Composizione e struttura di strati fosfatici microcristallini*, Bologna, Marzo 1983.
- (5) Hospadaruk V., J. Huff, R.W. Zurilla and H.T. Greenwood. Paint failure, steel surface, quality and accelerated corrosion testing. *SAE Paper* 780186 (1978).
- (6) Kamarchik P. and G.P. Cunningham. Applications of X-ray techniques to coatings analysis. *Progress in organic coatings*, 8 (1980), 81.
- (7) Kokubo J., S. Nomura, H. Sakai, M. Sakaguchi and M. Iwai. Newly developed Zn-Fe/Zn-Ni double-layer electroplated steel sheet. *SAE Paper* 830518 (1983).
- (8) Robin T.J., J. Durand, L. Cot, A. Bonnel, M. Duprat and F. Dabosi. Etude physicochimique et électrochimique de la protection d'un acier au carbone par le monofluorophosphates. I. Influence d'un traitement de conversion chimique. *J. App. Electrochem.*, 12 (1982), 701.
- (9) Hospadaruk V., and R.W. Zurilla. Qualitative test for zinc phosphate coating quality. *SAE Paper*, 780187 (1978).
- (10) Duffel, *Electroplating and metal finishing*, 7 (1954), 305.
- (11) ASTM standard method B117. Standard method of salt spray testing. *ASTM Book of Standards* (1982).
- (12) ASTM standard method B380. Standard method of corrosion testing of decorative chromium electroplating by the corrodkote procedure. *ASTM Book of Standards* (1982).
- (13) Davis J.W. The pretreatment of steel and galvanized steel for cathodic electrodeposition paint systems. *SAE Paper* 820336 (1982).
- (14) Van Loo M., D.D. Laiderman and R.R. Bruhn. Filiform corrosion. *Corrosion Nace*, 9 (1953), 277.